Neutron transfer reactions at large distances

K. E. Rehm, B. G. Glagola, W. Kutschera, F. L. H. Wolfs,* and A. H. Wuosmaa
Argonne National Laboratory, Argonne, Illinois 60439
(Received 23 October 1992)

^{58}Ni-induced one- and two-neutron transfer reactions have been measured on ^{232}Th at $E_{lab}=500$ MeV. The transfer probabilities at large internuclear distances measured for the deformed ^{232}Th target are compared with similar data on spherical ^{208}Pb. For one-neutron transfer reactions good agreement between experiment and the prediction from the tunneling model is observed in both cases. The transfer probabilities for two-neutron transfer reactions deviate from the semiclassical predictions. The disagreement increases at higher bombarding energies. These deviations can be explained by the influence of diffractive effects which become more important at higher bombarding energies.

PACS number(s): 25.70.Bc, 24.50.+g

I. INTRODUCTION

The study of nucleon transfer reactions at large internuclear distances has been an active field of research since it was first discussed by Breit, Hall, and Gluckstern 40 years ago [1]. At large distances, the influence of the distorting nuclear potential is generally small and the exchange of particles occurs via a quantum-mechanical tunneling process. In a plot of cross section vs distance of closest approach the transfer reactions exhibit an exponential falloff toward large distances, which, for neutron transfers, are governed by the binding energy of the transferred particle or particle clusters. A first comparison with experimental data for the ^{14}N(^{14}N,^{13}N)^{15}N system [2,3] showed good agreement between theoretical prediction and experiment.

In the following years a large number of heavy-ion-induced transfer reactions have been investigated and compared with the predictions of the tunneling theory [4–19] and, for the majority of cases, good agreement between experiment and theory has been observed. In some cases, however, serious deviations were found, which could not be explained within simple semiclassical theories. These deviations [6–8,11–14,17–19], which have been termed "slope anomalies" by some authors, can be grouped into three categories: (i) A large number of two-neutron transfer reactions exhibit exponential falloffs, which are not consistent with the predictions of the simple tunneling picture [6–8,11,13–18]. (ii) Oscillations in the cross section for two-neutron transfer reactions have been observed for Dy nuclei [12,17]. (iii) In one case involving one-neutron transfer reactions on deformed Sm nuclei, deviations from the theoretical slopes have been found [19].

While the first type of deviations has been observed in a large number of reactions, the other two seem to represent more complicated phenomena, since similar reactions on neighboring nuclei do not exhibit anomalous behavior [17,20].

It is the purpose of this paper to investigate some of these anomalies in more detail. For that purpose we have studied ^{58}Ni-induced one- and two-neutron transfer reactions on deformed ^{232}Th and compared the results to similar reactions on spherical ^{208}Pb at different bombarding energies.

II. EXPERIMENTAL DETAILS

Nucleon transfer at large distances can be studied by employing two different techniques. Since the influence of the nuclear potential is small, the distance of closest approach is given by the Rutherford value

$$D=\frac{Z_1Z_2e^2}{2E_{\text{c.m.}}}\left[1+\csc\left[\frac{\theta}{2}\right]\right], \tag{1}$$

where Z_1,Z_2 are the nuclear charges of the colliding nuclei, $E_{\text{c.m.}}$ the center-of-mass (c.m.) energy, and θ the c.m. scattering angle. For a given system D can thus be varied either by changing the incident energy with a detector located at a fixed angle θ (excitation function) or by varying the scattering angle θ at a fixed bombarding energy (angular distributions). In all these measurements it has to be kept in mind, however, that Eq. (1) is valid only if the influence of the nuclear potential can be neglected. Conditions for the validity of Eq. (1) will be discussed in Sec. III A. In the experiment described below, measurements of angular distributions were used to study nucleon transfer at large distances.

The experiments were performed with ^{58}Ni beams from the superconducting accelerator ATLAS. A 400-μg/cm^2 rolled ^{232}Th target mounted in the scattering chamber of the Enge split-pole spectrograph was bombarded by 500-MeV ^{58}Ni^{19+} ions. The outgoing particles were analyzed according to their magnetic rigidity and detected in a hybrid focal-plane detector consisting of a position-sensitive parallel-plate avalanche counter backed by a large Bragg-curve detector allowing single mass and Z resolu-

*Present address: NSRL, Department of Physics and Astronomy, University of Rochester, 271 East River Road, Rochester, NY 14627.

tion for particles up to Se [21]. Six charge states could be measured simultaneously with a given magnetic field setting, corresponding to about 90% of the total yield for reaction products with $Z=26-30$. For reaction products with $Z<26$ only a smaller part of the atomic charge state distribution was detected. The energy resolution of 2.5 MeV was determined mainly by the energy straggling in the thick ^{232}Th target. Inelastic scattering to low-lying states, which is expected to be strong for ^{232}Th could therefore not be separated from purely elastic scattering. Angular distributions for "elastic scattering" referred to in Sec. III A thus include contributions from inelastic scattering to excited states up to $E_x=5$ MeV.

III. EXPERIMENTAL RESULTS

A. Elastic scattering

To determine the internuclear distance at which the assumption of pure Rutherford trajectories breaks down, the cross section for elastic scattering in the system ^{232}Th+^{58}Ni (including inelastic excitation and normalized to the Rutherford cross section) is plotted in Fig. 1(a) (solid dots) as function of the radius parameter d_0, where d_0 is calculated by $D=d_0(A_1^{1/3}+A_2^{1/3})$. Also included are data obtained with Ti, Ni, and Se projectiles on ^{208}Pb and ^{154,144}Sm [22,23]. As can be seen from Fig. 1(a), these systems exhibit a universal behavior with σ_{el} remaining at its Rutherford value up to d_0 values of about 1.55 fm, followed by an exponential falloff at smaller radii. This indicates that the influence of the nuclear potential becomes important for distances corresponding to radii smaller than $1.55(A_1^{1/3}+A_2^{1/3})$.

It is interesting to investigate whether similar systematic behavior is observed also for lighter systems. Figure 1(b) shows a similar plot for three systems, involving ^{16}O, ^{28}Si, and ^{36}S projectiles [18,24,25] on ^{92}Mo and ^{208}Pb, respectively. To be consistent with the data of Fig. 1(a), inelastic excitations (which could be separated for these systems) were included in the definition of elastic scattering. As can be seen from Fig. 1(b) the radius parameter at which absorptive processes set in increases to about 1.65 fm for these systems. This means that for lighter systems the assumption of pure Rutherford trajectories breaks down at even larger distances.

An analysis of elastic scattering along the same lines has been performed previously by several other authors [9,26,27] with qualitatively similar results. For the very heavy system $U+U$ deviations from Rutherford scattering are observed for radius parameters $d_0<1.55$ fm [9]. In the analysis of Ref. [26] the falloff from the Rutherford cross sections for the systems ^{40}Ca, ^{40}Ar+^{208}Pb occurs at the radius parameter $d_0=1.5$ fm. In this case, however, quasielastic transfer channels were included in the definition of the elastic cross sections, which leads to a shift of the distribution towards smaller d_0 values by about 0.1 fm [22].

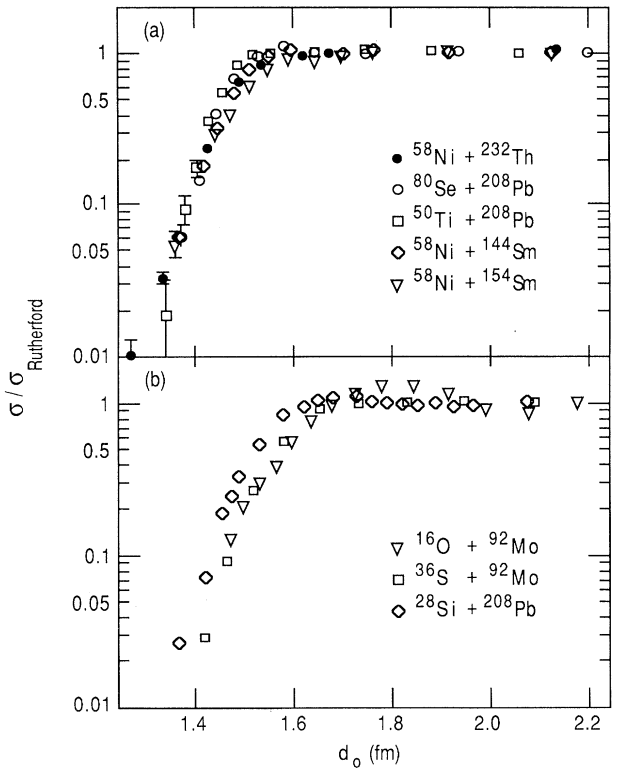

FIG. 1. (a) Cross section for elastic scattering (including inelastic excitation up to 5 MeV) normalized to the corresponding Rutherford value plotted as function of the reduced radius parameter d_0 for the systems ^{58}Ni+^{232}Th, ^{80}Se, ^{50}Ti+^{208}Pb, and ^{58}Ni+^{144,154}Sm. (b) Same as (a) but for the systems ^{28}Si+^{208}Pb, and ^{16}O,^{36}S+^{92}Mo.

B. Transfer reactions

The good particle identification of the detection system permitted measurement of angular distributions for a variety of reaction products ranging from Ti to Ni. The angular distributions for reaction products with different nuclear charges Z are given in Fig. 2. As observed previ-

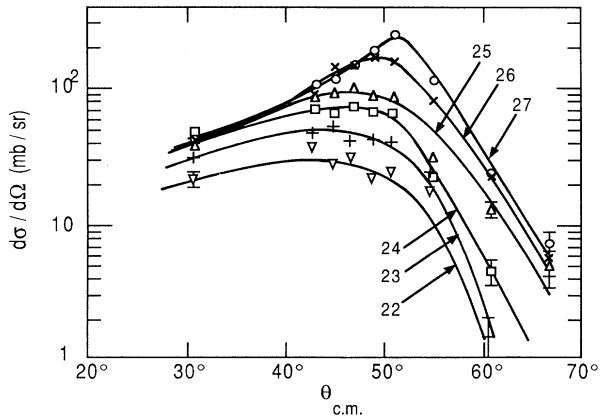

FIG. 2. Angular distributions for ^{58}Ni-induced transfer reactions on ^{232}Th at $E_{lab}=500$ MeV leading to ejectiles with different nuclear charge Z. The solid lines serve to guide the eye.

TABLE I. Angle-integrated reaction cross sections for reaction products with different nuclear charge Z. The values quoted for $Z<26$ are not corrected for efficiency and represent lower limits only. The total reaction cross section was taken from the measured quarterpoint angle and the cross section for quasifission events was obtained from an interpolation of the data from Ref. [29].

Z	σ (mb)
20	20
21	45
22	70
23	100
24	140
25	170
26	240
27	290
28	360
29	70
σ_{transfer}	1505
$\sigma_{\text{fusion-fission}}$	800
σ_{react}	2500

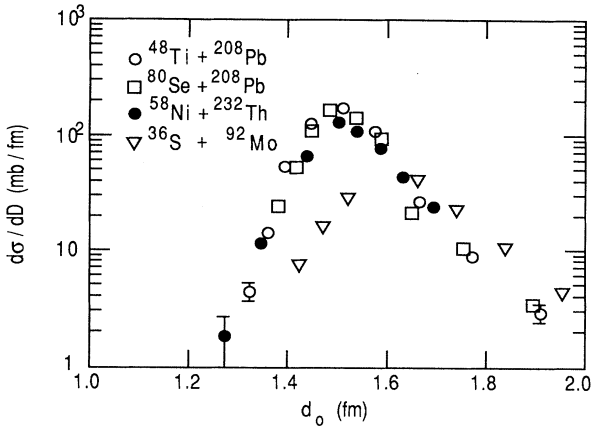

FIG. 4. $d\sigma/dD$ plotted as function of the reduced radius parameter d_0 for the one-neutron transfer reaction ^{232}Th(^{58}Ni,^{59}Ni)^{231}Th (solid points) in comparison with ^{80}Se-, ^{48}Ti-, and ^{36}S-induced one-neutron pickup reactions on various spherical nuclei.

ously for other systems the maximum of the distributions shifts to more forward angles for reactions involving large charge transfers. The angle-integrated cross section for these transfer reactions (not corrected for the reduced efficiency for $Z<26$) are summarized in Table I together with the total reaction cross section obtained from the quarter-point angle $\theta_{1/4}$ [28] and the cross section for quasifission, which was interpolated from a systematic study of ^{238}U on various light and medium mass nuclei in Ref. [29]. The measured yield for the sum of transfer and fusion-fission processes is smaller than the total reaction cross section because of the reduced particle detection efficiency for nuclei further away from $Z=28$.

The large cross sections for the neutron transfer reactions (^{58}Ni, ^{57,59,60}Ni) allowed an analysis of the mass

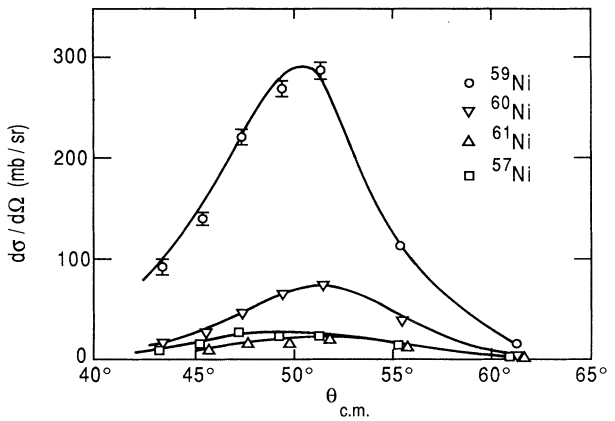

FIG. 3. Angular distributions for the neutron transfer reactions ^{232}Th(^{58}Ni,^{57,59,60,61}Ni)^{233,231,230,229}Th at $E_{\text{lab}}=500$ MeV. The solid lines serve to guide the eye.

separated $Z=28$ reaction products. The resulting angular distributions are shown in Fig. 3. The angle-integrated cross sections of 26±5 mb (^{57}Ni), 250±30 mb (^{59}Ni), 63±12 mb (^{60}Ni), and 20±5 mb (^{61}Ni) agree well with the systematics of Ref. [30].

It is interesting to compare the shape of the angular distribution for the one-neutron transfer reaction obtained in this experiment with the results of the same reactions on spherical ^{208}Pb. In Fig. 4 $d\sigma/dD$ is plotted vs the reduced radius parameter $d_0=D/(A_1^{1/3}+A_2^{1/3})$ for the one-neutron transfer reaction ^{232}Th (^{58}Ni, ^{59}Ni)^{231}Th (solid points) and three other one-neutron transfer induced by ^{36}S [18], ^{48}Ti [31], and ^{80}Se [30] on ^{92}Mo and ^{208}Pb, respectively. For the reactions involving heavier projectiles and targets the maximum of the transfer cross section occurs at a radius parameter $d_0=1.5$ fm, whereas the maximum for the lighter system ^{36}S+^{92}Mo is shifted to $d_0=1.65$ fm. These observations for the transfer reactions are consistent with the results obtained from the data for elastic scattering, which also show a larger critical radius parameter for the lighter system.

IV. DISCUSSION

A. Transfer probabilities for spherical and deformed nuclei

The transfer of nucleons at larger distances is best discussed by introducing the so-called transfer probability P_t. P_t can be defined as

$$P_t=\frac{d\sigma_{\text{tr}}}{2\pi b\,db}\,, \tag{2}$$

where $d\sigma_{\text{tr}}$ is the transfer cross section at a given scattering angle θ and b is the impact parameter associated with this scattering angle. Using the Rutherford values for the impact parameter b, P_t can be transformed into

$$P_t = \frac{d\sigma_{\rm tr}}{d\sigma_{\rm Ruth}} \ . \tag{3}$$

Since at large distances the overlap of the two nuclei is small, the wave function of the transferred nucleon can (for neutron transfer) be approximated by a Hankel function resulting in a semiclassical expression for P_t [32]:

$$P_t \sim \sin\frac{\theta}{2} \exp(-2\alpha D) \ . \tag{4}$$

In Eq. (4) D is the classical expression for the distance of closest approach [see Eq. (1)]. For a transfer reaction $A(a,a+1)A-1$ α can be calculated from the binding energy B_A of the neutron in nucleus A:

$$\alpha = \frac{\sqrt{2\mu B_A}}{\hbar} \ . \tag{5}$$

In Eq. (5) μ is the reduced mass of the neutron in nucleus A. The solid points in Fig. 5 show $P_t/\sin(\theta/2)$ plotted vs the distance of closest approach D for the one-neutron transfer reaction ^{232}Th(^{58}Ni,^{59}Ni)^{231}Th. The arrow indicates the critical radius calculated with a radius parameter $d_0 = 1.55$ fm. The solid line for larger distances is obtained from a least-squares fit to the data and the slope parameter agrees quite well with the value calculated from Eq. (5).

In some cases different definitions of the transfer probability have been used:

$$P_t = \frac{d\sigma_{\rm tr}}{d\sigma_{\rm el}}, \quad P_t = \frac{d\sigma_{\rm tr}}{d\sigma_{\rm Ruth}(1-P_a)} \ , \tag{6}$$

where either the Rutherford cross section has been replaced by the cross section for elastic scattering or an absorption function P_a has been introduced. P_a is usually obtained from the falloff of the angular distribution for elastic scattering. The results of using Eq. (6) for the calculation of P_t are shown as open points in Fig. 5. It can be seen that the transfer probability now exhibits two contributions with a much shallower falloff observed for distances below about 15 fm. It is obvious that if no data would have been available at large distances, the wrong slope would be obtained using Eq. (6). Although Eq. (6) has been used in a larger number of experimental studies, there are several difficulties. (i) In many cases the definition of $\sigma_{\rm el}$ includes inelastic channels that effect the slope parameter extracted from data at smaller distances. (ii) At larger nuclear overlaps the distance of closest approach cannot be calculated from Eq. (1). Calculations [33] of the distance of closest approach D for the system ^{86}Kr+^{208}Pb including the influence of the nuclear potential which, because of its imaginary part is mainly repulsive, showed that the actual distance is larger than the Rutherford value by up to 1 fm. This effect thus leads to an additional uncertainty in the slope determination for data obtained at distances smaller than the ones calculated with $d_0 = 1.55$ fm. In the following we will therefore, only consider data that are measured at internuclear distances where the assumption of pure Rutherford trajectories is well justified.

The transfer probabilities $P_t/\sin(\theta/2)$ for the strongest neutron transfer reactions ^{232}Th (^{58}Ni,^{59,60}Ni)^{231,230}Th plotted as function of the reduced radius parameter d_0 are shown in Fig. 6 together with similar data measured

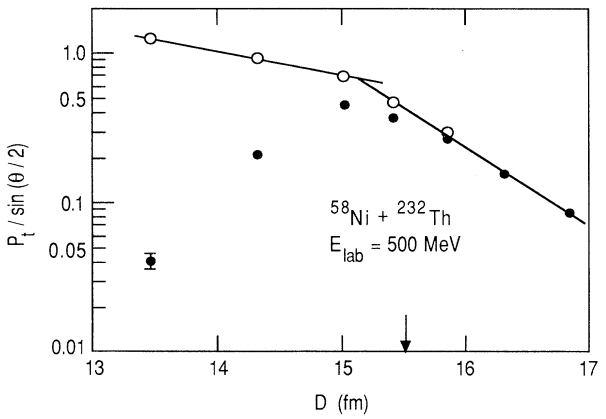

FIG. 5. Transfer probability $P_t/\sin(\theta/2)$ plotted as function of the distance of closest approach for the reaction ^{232}Th(^{58}Ni,^{59}Ni)^{231}Th at $E_{\rm lab} = 500$ MeV (solid points). The open circles are obtained using a different definition of the transfer probability P_t (see text for details). The solid lines are obtained from least-squares fits to the data and correspond to slope constants of 0.36 ± 0.03 fm^{-1} (for $D < 15.2$ fm) and 1.15 ± 0.06 fm^{-1} (for $D > 15.5$ fm), respectively.

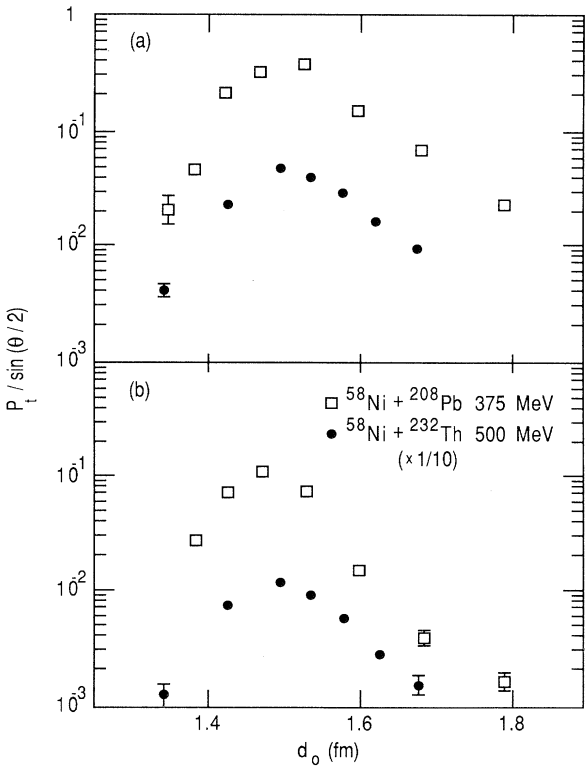

FIG. 6. (a) $P_t/\sin(\theta/2)$ plotted as function of the radius parameter d_0 for the one-neutron transfer reaction (^{58}Ni,^{59}Ni) on ^{232}Th (solid points) and ^{208}Pb (open squares), respectively. (b) Same as (a) but for the two-neutron transfer reaction (^{58}Ni,^{60}Ni).

TABLE II. Slope parameters for the transfer probability $P_t/\sin(\theta/2)$ obtained from least-squares fits to data measured at distances $D > 1.55\ (A_1^{1/3}+A_2^{1/3})$ for one- and two-neutron transfer reactions induced by ^{58}Ni on ^{232}Th and ^{208}Pb.

Reaction	E_{lab} (MeV)	$2\alpha_{expt}$ (fm^{-1})	$2\alpha_{theor}$ (fm^{-1})	$\alpha_{expt}/\alpha_{theor}$
^{232}Th(^{58}Ni,^{59}Ni)	500	1.15±0.06	1.11	1.04±0.05
^{232}Th(^{58}Ni,^{57}Ni)	500	1.46±0.2	1.52	0.96±0.13
^{208}Pb(^{58}Ni,^{59}Ni)	375	1.08±0.09	1.19	0.91±0.08
^{232}Th(^{58}Ni,^{60}Ni)	500	1.36±0.08	2.10	0.65±0.04
^{208}Pb(^{58}Ni,^{60}Ni)	375	1.95±0.11	2.32	0.84±0.05

for ^{208}Pb at $E_{lab}=375$ MeV [22]. The slopes obtained for the one- and two-neutron transfer reactions from least-squares fits to data points with $d_0 > 1.55$ fm are summarized in Table II. The cross sections for ^{208}Pb(^{58}Ni,^{57}Ni)^{209}Pb were too small to deduce a reliable slope parameter for this reaction. For the one-neutron transfer reactions the results of Table II exhibit a good agreement between the experimental data and the theoretical predictions obtained from Eq. (5). This is in contrast with the observations of Ref. [19] where at subbarrier energies smaller slopes were obtained for the (^{58}Ni,^{59}Ni) transfer reaction on deformed Sm isotopes, while for the spherical ^{144}Sm the expected falloff for the transfer probability was observed. It is not clear if this discrepancy is caused by experimental effects (e.g., different charge state distributions due to isomeric states) or by a nuclear structure effect, which is present only for Sm isotopes, since similar preliminary measurements on Dy isotopes did not show any anomalous slope parameters for the one-neutron transfer reactions [20]. Also, data for ^{58}Ni+^{144,154}Sm measured at energies above the Coulomb barrier [23] did not show any anomalies. Similarly ^{16}O-induced one- and two-neutron pickup reactions measured at the Coulomb barrier [34] were in good agreement with the slope parameters calculated by Eq. (5).

While the slopes of the transfer probability for the one-neutron transfer reactions studied in this experiment are in good agreement with the theoretical predictions, deviations are observed for the two-neutron case. The ratio between experimental and theoretical slope parameters reaches values as small as 0.65 for the reaction ^{232}Th(^{58}Ni,^{60}Ni)^{230}Th. Possible causes for this behavior will be discussed in the following sections.

B. System and energy dependence of the transfer probabilities

In order to shed some light on the possible origin of the slope anomaly for two-neutron transfer reactions [6–8,11,14–18] the data obtained from the present measurement have been compared with results from similar studies performed on a variety of different target nuclei [22,23,35]. All data were obtained from angular distributions and were analyzed along similar lines as discussed in Sec. IV A. The ratio of the experimental and predicted slope parameters for the one-neutron pickup reaction induced by ^{58}Ni on different target nuclei with mass A are shown in Fig. 7(a) and generally good agreement between theory and experiment is observed.

The ratios for the two-neutron pickup reactions are shown in Fig. 7(b). For the majority of the data the experimental slopes are smaller than expected assuming either the tunneling of a two-neutron cluster or a successive transfer of two neutrons [4,5]. No special nuclear mass dependence is observed.

While most of these measurements were performed at a single energy, (typically 10–30 % above the Coulomb barrier), data obtained at different bombarding energies ranging from the Coulomb barrier to $E/V_C=1.8$ exist for the system ^{58}Ni+^{208}Pb [22,35]. The slope parameters 2α observed for the one- and two-neutron pickup reactions (^{58}Ni,^{59,60}Ni) plotted as function of E/V_C with V_C calculated from the quarter-point angle $\theta_{1/4}$ are shown in Fig. 8. The dotted lines are the theoretical slopes calcu-

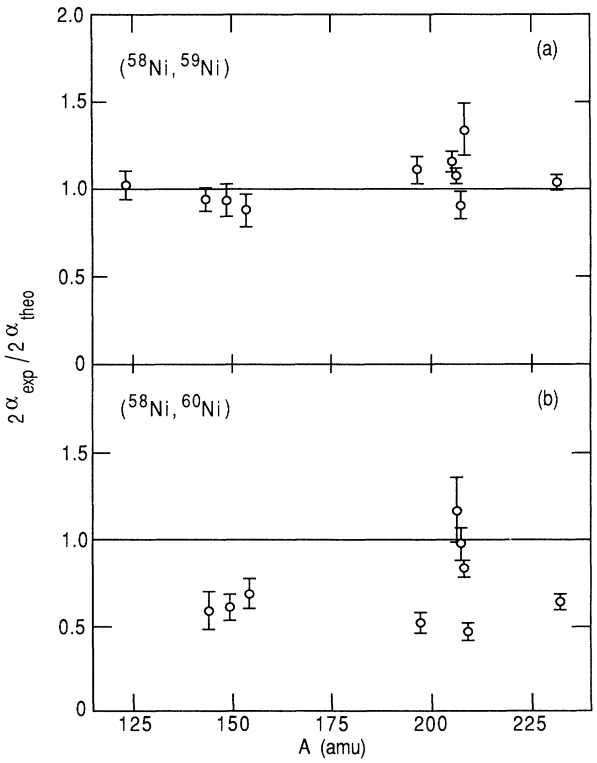

FIG. 7. (a) Ratio of the experimental slope parameters $2\alpha_{expt}$ and the theoretical values for the one-neutron pickup reaction (^{58}Ni,^{59}Ni) on various target nuclei with mass A. (b) Same as (a) but for the two-neutron transfer reaction (^{58}Ni,^{60}Ni).

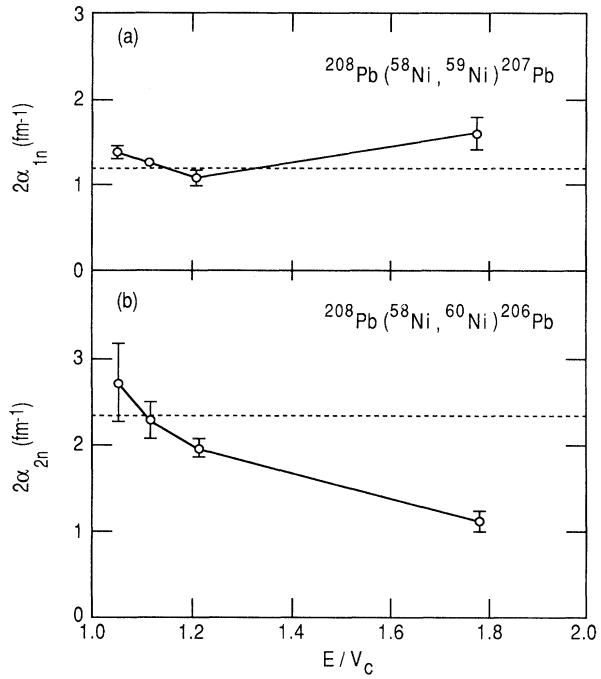

FIG. 8. (a) Experimental slope parameters 2α for the one-neutron transfer reaction ^{208}Pb(^{58}Ni,^{59}Ni)^{207}Pb as function of the energy above the Coulomb barrier E/V_C. The dotted line is the theoretical slope calculated from the corresponding binding energy. (b) Same as (a), but for the two-neutron transfer ^{208}Pb(^{58}Ni,^{60}Ni)^{206}Pb.

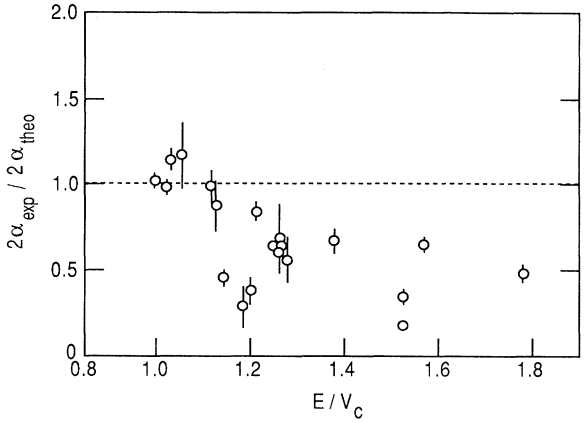

FIG. 9. Ratio of the experimental slope parameter $2\alpha_{expt}$ and the theoretical values calculated from Eq. (5) as function of the energy above the Coulomb barrier E/V_C for two-neutron transfer reactions induced by projectiles ranging from ^{36}S to ^{64}Ni on different target nuclei.

lated from Eq. (5). While the slopes for the one-neutron transfer reactions are in reasonable agreement for all energies the expected theoretical slope parameters for the two-neutron transfer reactions (about twice as steep as for the one-neutron transfer reactions) are obtained only at energies in the vicinity of the Coulomb barrier. This observation is consistent with similar results for the system ^{28}Si+^{208}Pb, which produce the correct slope parameter only at low bombarding energies [25,36–38]. An explanation of this energy dependence is presented in the following section.

V. THEORETICAL INTERPRETATIONS

The energy dependence of the slope parameter for two-neutron transfer reactions is not limited to the ^{58}Ni+^{208}Pb and ^{28}Si+^{208}Pb cases. Figure 9 shows the ratios of the experimental slope parameter divided by the theoretical values ($2\alpha_{2n}$) expected from the simple tunneling picture plotted as function of the energy above the Coulomb barrier E/V_C for different systems ranging from ^{36}S+^{58}Ni to ^{58}Ni+^{232}Th. A compilation of the data is given in Table III. Only data obtained at distances corresponding to radius parameters $d_0 > 1.55$ fm have been included. As seen from Fig. 9 good agreement between the experimental and theoretical slopes is observed only at energies in the vicinity of the Coulomb barrier. At energies above the barrier large fluctuations are obtained for the different systems.

In order to gain a better understanding of this energy and system dependence the applicability of the semiclassical model needs to be investigated. Several authors have discussed the conditions under which the scattering process can be described within the concept of classical trajectories [32,40–43]. The critical parameters in all these calculations is the width of the partial wave distribution Δl. It is shown in Ref. [32] that a treatment of the scattering process within classical dynamics requires a width of the partial wave distribution, which is larger than a critical value Δl_c given by

$$\Delta l_c = \frac{\sqrt{\eta}}{\sin(\theta_0/2)} , \tag{7}$$

where η is the Sommerfeld parameter and θ_0 the scattering angle associated with the maximum of the angular distribution.

Δl_c can be translated into a limit for the width of the form factor ΔD_c:

$$\Delta D_c = \left[\hbar D_0 \left[\frac{2}{\mu V_C} \right]^{1/2} \frac{(E/V_C - 1)}{\sqrt{E/V_C}} \right]^{1/2} , \tag{8}$$

where D_0 is the distance of closest approach at the angle θ_0, μ the reduced mass, and V_C the Coulomb barrier.

The requirements for a semiclassical treatment are that the width of the l distribution (or the form factor) is larger than the critical values given by Eqs. (7) and (8). Reaction processes involving very localized form factors or l distributions, on the other hand, lead to quantal diffraction processes and the use of classical trajectories is not justified anymore.

As can be seen from Eq. (8) the requirement of $\Delta D > \Delta D_c$ is easily fulfilled for energies in the vicinity of the Coulomb barrier where ΔD_c approaches zero. At energies above the Coulomb barrier small values of ΔD_c are obtained for systems involving heavy nuclei with high nuclear charge Z.

TABLE III. Ratios between the experimental slope parameters $2\alpha_{expt}$ and the theoretical values for various two-neutron transfer reactions shown in Fig. 9.

Reaction	Target	E_{lab}	E/V_C	$2\alpha_{expt}/2\alpha_{theor}$	Ref.
(^{36}S,^{34}S)	^{58}Ni	112	1.14	0.46	[39]
(^{32}S,^{34}S)	^{64}Ni	109	1.20	0.38	[39]
(^{36}S,^{34}S)	^{92}Mo	140	1.18	0.29	[18]
		180	1.52	0.18	[18]
(^{58}Ni,^{60}Ni)	^{144}Sm	<275[a]	1.00	1.02	[19]
		343	1.26	0.68	[23]
	^{154}Sm	337	1.28	0.56	[23]
(^{120}Sn,^{118}Sn)	^{112}Sn	550	1.02	0.98	[10]
(^{28}Si,^{30}Si)	^{208}Pb	152	1.03	1.15	[36]
		166	1.13	0.88	[36]
		225	1.52	0.35	[25]
(^{37}Cl,^{39}Cl)	^{208}Pb	250	1.38	0.67	[22]
(^{46}Ti,^{48}Ti)	^{208}Pb	297	1.25	0.63	[31]
(^{48}Ti,^{50}Ti)	^{208}Pb	300	1.26	0.61	[31]
(^{50}Ti,^{52}Ti)	^{208}Pb	303	1.27	0.63	[31]
(^{58}Ni,^{60}Ni)	^{208}Pb	325	1.05	1.18	This work
		345	1.12	0.98	This work
		375	1.21	0.84	This work
		550	1.78	0.48	This work
(^{58}Ni,^{60}Ni)	^{232}Th	500	1.57	0.65	This work

[a]The data were obtained from an excitation function at sub-barrier energies and are plotted at $E/V_C=1.0$.

In order to study the influence of the width of the form factor in more detail calculations have been performed for the system ^{58}Ni+^{232}Th using the partial wave expression for the cross section:

$$\frac{d\sigma}{d\Omega}=\left|\frac{1}{2ik}\sum_l(2l+1)a_l e^{2i\sigma_l}P_l(\cos\theta)\right|^2 . \quad (9)$$

In Eq. (9) σ_l is the Coulomb phase shift, a_l the parametrized form factor, and P_l the Legendre polynomial of order l. For a study of the one-neutron transfer reaction the shape of a_l was taken from an exact finite-range distorted wave Born approximation calculation using the code PTOLEMY [44] [see solid line in Fig. 10(a)]. The resulting transfer probability [divided by $\sin(\theta/2)$] is shown as a solid line in Fig. 10(b) and exhibits a slope of 1.21 fm^{-1} in good agreement with the value calculated from the binding energy of one neutron in ^{232}Th (1.11 fm^{-1}). The width of the form factor for one-neutron transfer is larger than the critical width calculated from Eq. (7), which is shown as the solid bar in Fig. 10(a). Increasing the slope of the form factor [see dashed line in Fig. 10(a)] results in a steeper falloff of the transfer probability as seen from the corresponding curve in Fig. 10(b). This statement holds as long as the width of a_l is larger than Δl_c. Form factors with a very small width in l space [dotted curve in Fig. 10(a)] result in transfer probabilities that show the same slope parameter as observed for the one-neutron transfer reaction. The form factors extracted from the measured transfer probabilities for the system ^{58}Ni+^{232}Th are shown in Fig. 11. Similar to a previous analysis [18] for the system ^{36}S+^{92}Mo it is observed that the width of the two-neutron transfer form factor is considerably smaller than for the one-neutron case.

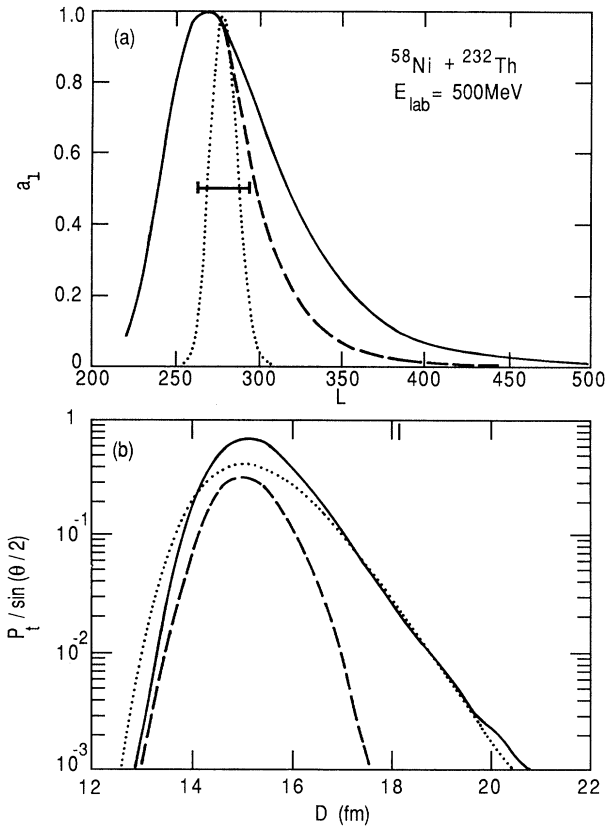

FIG. 10. Form factors (top) and the resulting transfer probabilities (bottom) calculated from Eq. (9) for the system ^{58}Ni+^{232}Th at $E_{lab}=500$ MeV. The form factors have been arbitrarily normalized to 1 at their maximum value (see text for details).

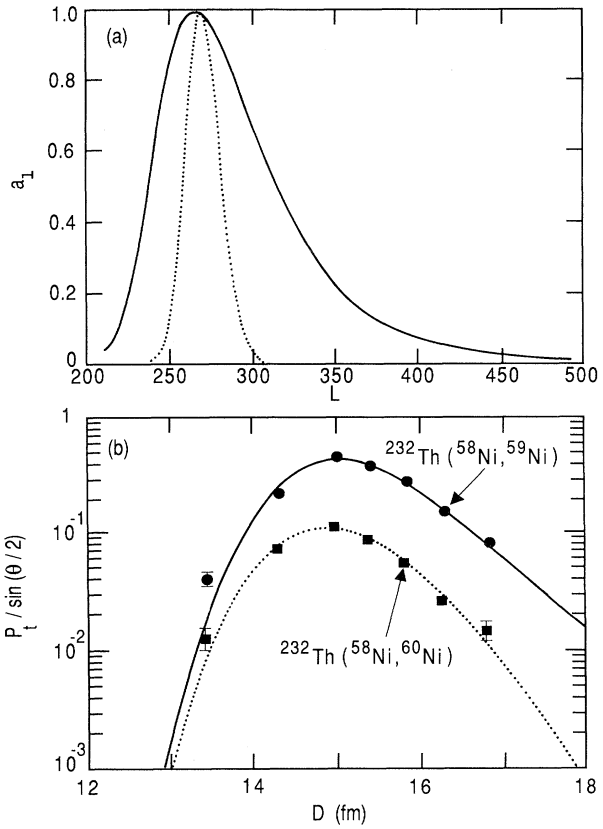

FIG. 11. Form factors for one- and two-neutron transfer reactions in the system ^{58}Ni+^{232}Th (top) extracted from the measured transfer probabilities (bottom).

These examples show that deviations from the expected slopes in the transfer probabilities do not necessarily indicate a breakdown of the tunneling picture but can also arise from a change in the reaction mechanism, such as the introduction of two-step process, which, as shown in Ref. [45], have much more localized form factors. These deviations are expected mainly at higher bombarding energies. At energies at or below the Coulomb barrier the tunneling description should be valid, independent of the shape of the form factor as long as Eq. (7) is fulfilled. The experimental data shown in Fig. 9 confirm this observation.

VI. SUMMARY AND CONCLUSION

The question of so-called anomalous slope parameters for nucleon transfer at large distances has been investigated. For ^{58}Ni-induced one-nucleon transfer reactions on deformed ^{232}Th no anomalies have been observed. The falloff for the transfer probability toward large distances is in good agreement with the theoretical expectations calculated within the tunneling model for both deformed ^{232}Th and spherical ^{208}Pb.

Many of the anomalies quoted in the literature are caused by the inapplicability of the semiclassical model. Despite the apparent success of the semiclassical model in many reactions, the domain of applicability of this approximation should not be overlooked. Data from excitation functions measured at sub-barrier energies are usually in good agreement with the predictions of the simple tunneling picture because, as outlined in Sec. V, the assumption of classical trajectories is well justified. Data obtained at energies above the Coulomb barrier must be interpreted more carefully. A large number of experiments include data where the two nuclei experience a considerable overlap and thus the assumption of Rutherford trajectories is not justified. Due to the onset of absorption, the effective distances of closest approach are generally larger than the corresponding Rutherford values. Values of the slope parameters extracted under these conditions should therefore be considered with caution.

Restricting the analysis of the data to large internuclear distances can eliminate some of the problems; however, the question about the applicability of the semiclassical model still remains. If the width of the form factor is smaller than a critical value given in Sec. V, the assumption of classical trajectories is no longer justified and the analysis must be performed within the diffraction model. Slope parameters extracted from transfer probabilities for systems that fulfill the necessary criteria for the applicability of a semiclassical treatment are generally in good agreement with the theoretical predictions.

This work was supported by the U.S. Department of Energy, Nuclear Physics Division, under Contract No. W-31-109-ENG-38.

[1] G. Breit, M. H. Hall, Jr., and R. L. Gluckstern, Phys. Rev. **87**, 74 (1952).
[2] G. Breit and M. E. Ebel, Phys. Rev. **103**, 679 (1956).
[3] J. C. Hiebert, J. A. McIntyre, and J. G. Couch, Phys. Rev. **138**, B346 (1965).
[4] W. von Oertzen, in *Proceedings of the Workshop on the Interface between Nuclear Structure and Heavy Ion Reaction Dynamics (Notre Dame, Indiana, 1990)*, edited by R. R. Betts and J. J. Kolata, Institute of Physics Conference Series 109 (IOP, Bristol, 1991), and references therein.
[5] W. von Oertzen, B. Gebauer, A. Gamp, H. G. Bohlen, F. Busch, and D. Schüll, Z. Phys. A **313**, 189 (1983).
[6] G. Himmele, H. Backe, P. A. Butler, D. Habs, V. Metag, and J. B. Wilhelmy, Nucl. Phys. **A404**, 401 (1983).
[7] A. O. Machiavelli, M. A. Deleplanque, R. M. Diamond, F. S. Stephens, E. L. Dines, and J. E. Draper, Nucl. Phys. **A432**, 436 (1985).
[8] K. Sapotta, R. Bass, U. Hartmann, H. Noll, R. E. Renfordt, and K. Stelzer, Phys. Rev. C **31**, 1297 (1985).
[9] G. Wirth, Phys. Lett. B **177**, 286 (1986).
[10] W. von Oertzen, M. G. Bohlen, B. Gebauer, R. Künkel, F. Pühlhofer, and D. Schüll, Z. Phys. A **326**, 463 (1987).
[11] F. W. N. de Boer, H. J. Wollersheim, H. Emling, H. Grein, E. Grosse, W. Spreng, G. Eckert, T. W. Elze, K. Stelzer, and Ch. Lauterback, Z. Phys. A **325**, 457 (1987).
[12] C. Y. Wu, X. T. Liu, W. J. Kernan, D. Cline, T. Czosny-

ka, M. W. Guidry, A. E. Kavka, R. W. Kincaid, B. Kotlinski, S. P. Sorensen, and E. Vogt, Phys. Rev. C **39**, 298 (1989).

[13] S. Yuutinen, X. Y. Liu, S. Sòrensen, B. Cox, R. W. Kincaid, C. R. Bingham, M. W. Guidry, W. J. Kernan, C. Y. Wu, E. Vogt, T. Czosnyka, D. Cline, M. L. Halbert, I. Y. Lee, and C. Baktash, Phys. Lett. B **192**, 307 (1987).

[14] J. Gerl, W. Körten, D. Habs, D. Schwalm, and H. J. Wollersheim, Z. Phys. A **334**, 195 (1989).

[15] C. N. Pass, P. M. Evans, A. E. Smith, L. Stuttgé, R. R. Betts, J. S. Lilley, D. W. Banes, K. A. Connell, J. Simpson, J. R. Smith, A. N. James, and B. R. Fulton, Nucl. Phys. **A499**, 173 (1989).

[16] L. Corradi, S. J. Skorka, U. Lenz, K. E. G. Löbner, P. R. Pascholati, U. Onade, K. Rudolph, W. Schomburg, M. Steinmayer, H. G. Thies, G. Montagnolil, D. R. Napoli, A. M. Stefanini, A. Tivelli, S. Beghini, F. Scarlassara, C. Signorini, and F. Soramel, Z. Phys. A **355**, 55 (1990).

[17] W. J. Kernan, C. Y. Wu, X. T. Liu, X. L. Han, D. Cline, T. Czosnyka, M. W. Guidry, M. L. Halbert, S. Justinen, A. E. Kavka, R. W. Kincaid, J. O. Rasmussen, S. P. Sorensen, M. A. Stoyer, and E. G. Vogt, Nucl. Phys. **A524**, 344 (1991).

[18] A. H. Wuosmaa, K. E. Rehm, B. G. Glagola, Th. Happ, W. Kutschera, and F. L. H. Wolfs, Phys. Lett. B **255**, 316 (1991).

[19] R. R. Betts, in *Proceedings of the JAERI International Symposium, Hitachi, 1988,* edited by Y. Sugiyama, A. Iwamoto, and H. Ikezoe (Japan Universal Academy Press, Tokyo, 1989); R. R. Betts, in *Proceedings of the Symposium Heavy Ion Interactions around the Coulomb Barrier, Legnaro, 1988,* edited by C. Signorini, S. Skorka, P. Spolaore, and A. Vitturi, Lecture Notes in Physics, Vol. 317 (Springer-Verlag, Berlin, 1988).

[20] J. S. Lilley, M. J. Smithson, R. R. Betts, A. E. Smith, A. N. James, and M. Freer, Daresbury Annual Report 1989/1990, ISSN: 0265-1815 (unpublished).

[21] K. E. Rehm and F. L. H. Wolfs, Nucl. Instrum. Methods A **273**, 262 (1988).

[22] K. E. Rehm, D. G. Kovar, W. Kutschera, M. Paul, G. S. F. Stephans, and J. L. Yntema, Phys. Rev. Lett. **51**, 1426 (1983).

[23] A. M. van den Berg, K. E. Rehm, D. G. Kovar, W. Kutschera, and G. S. F. Stephans, Phys. Lett. B **194**, 334 (1987).

[24] K. E. Rehm, H. J. Körner, M. Richter, H. P. Rother, J. P. Schiffer, and H. Spieler, Phys. Rev. C **12**, 1945 (1975).

[25] J. J. Kolata, K. E. Rehm, D. G. Kovar, G. S. F. Stephans, G. Rosner, H. Ikezoe, and R. Vojtech, Phys. Rev. C **30**, 125 (1984).

[26] Y. T. Oganessian, Y. E. Penionzhkevich, V. I. Man'ko, and U. N. Polyansky, Nucl. Phys. **A303**, 259 (1978).

[27] W. von Oertzen, in Proceedings of the International School of Physics "Enrico Fermi," Course CXII, Varenna, 1989, edited by C. Detraz and P. Kienle (North-Holland, Amsterdam, 1991).

[28] W. E. Frahn, Nucl. Phys. **A302**, 267 (1978).

[29] W. Q. Shen, J. Albinski, A. Gobbi, S. Gralla, K. D. Hildenbrand, N. Hermann, J. Kuzminski, W. F. J. Müller, H. Stelzer, J. Toke, B. B. Back, S. Bjornholm, and S. P. Sorensen, Phys. Rev. C **36**, 115 (1987); B. Back, private communication.

[30] K. E. Rehm, C. Beck, A. van den Berg, D. G. Kovar, L. L. Lee, W. C. Ma, F. Videbaek, M. Vineyard, and T. F. Wang, Phys. Rev. C **42**, 2497 (1990).

[31] K. E. Rehm, A. M. van den Berg, J. J. Kolata, D. G. Kovar, W. Kutschera, G. Rosner, G. S. F. S. Stephans, and J. L. Yntema, Phys. Rev. C **37**, 2629 (1988).

[32] R. Bass, *Nuclear Reactions with Heavy Ions* (Springer, Berlin, 1980).

[33] E. Vigezzi and A. Winther, Ann. Phys. (N.Y.) **192**, 431 (1989).

[34] Y. Sugiyama, J. Tomita, H. Ikezoe, K. Idendo, N. Kato, T. Sugimitsu, and H. Fujita, Annual Report of JAERI Tandem Linac 1989 (unpublished).

[35] K. E. Rehm, Annu. Rev. Nucl. Part. Sci. **41**, 429 (1991).

[36] R. J. Vojtech, J. J. Kolata, L. A. Lewandowski, K. E. Rehm, D. G. Kovar, G. S. F. Stephans, G. Rosner, H. Ikezoe, and M. F. Vineyard, Phys. Rev. C **35**, 2139 (1987).

[37] R. J. Vojtech, Ph.D. thesis, University of Notre Dame, 1987 (unpublished).

[38] K. E. Rehm, in *Proceedings of the XII Workshop on Nuclear Physics, Iguazu Falls, Argentina, 1989,* edited by M. C. Cambiaggio, A. J. Kreiner, and E. Ventura (World Scientific, Singapore, 1990).

[39] A. M. Stefanini, G. Montagnoli, G. Fortuna, R. Menegazzo, S. Beghini, C. Signorini, A. DeRosa, G. Inglima, M. Sandoli, F. Rizzo, G. Pappalardo, and G. Cardella, Phys. Lett. **185**, 15 (1987), and private communication.

[40] V. M. Strutinski, Zh. Eksp. Teor. Fiz. **46**, 2078 (1964) [Sov. Phys. JETP **19**, 1401 (1964)]; Phys. Lett. **44B**, 245 (1973).

[41] H. L. Harney, P. Braun-Munzinger, and C. K. Gelbke, Z. Phys. A **269**, 339 (1974).

[42] R. A. Broglia and A. Winter, Phys. Lett. C **4**, 153 (1972).

[43] P. J. Siemens and F. D. Becchetti, Phys. Lett. **42B**, 389 (1972).

[44] M. H. Macfarlane and S. C. Pieper, Argonne National Laboratory Report No. ANL-76-11 (Rev. 1), 1978 (unpublished).

[45] R. J. Ascuitto and E. A. Seglie, in *In Treatise on Heavy Ion Science Vol. I,* edited by D. A. Bromley (Plenum, New York, 1984).